Lawal, S.A., Ndaliman, M.B., Bala, K.C., and Lawal, S.S. (2017) Effect of Cutting Variables on Boring Process: A Review. In: Hashmi, M.S.J. (ed.), Comprehensive Materials Finishing. vol. 1, pp. 26–46. Oxford: Elsevier.

1.2 Effect of Cutting Variables on Boring Process: A Review

SA Lawal, MB Ndaliman, KC Bala, and SS Lawal, Federal University of Technology, Minna, Nigeria

1.2.1 Introduction

Boring is a process of enlarging a hole size that was already made by drilling, or casting to the designed dimension. The enlargement of hole can be made by means of a single point cutting tool or a boring head containing multiple tools. The boring of an engine cylinder or of a gun barrel is an example of such process. In boring, either the boring head/bar can be rotated or the workpart can be rotated. Boring machines or boring mills usually rotate the boring bar against a stationary workpiece. Also in turning machines, boring can be performed where the boring bar attached to the tool post remains stationary against a rotating workpiece held in the lathe chuck. The boring bar with insert attached to it is fed into an existing hole. Depending on material, type of tool insert, and cutting conditions, the chip formed may either be continuous or discontinuous. The surface produced is known as bore. Surface roughness in boring may vary between 0.0002 and 0.006 mm. With the advancement of machining technology, the limitations of boring with respect to geometric accuracy and material hardness have been diminishing. With new grades of carbide and ceramic tool inserts, the accuracy of boring and surface quality has increased. The hole produced may either be straight or tapered. The work holding devices used lathe could be either three-jaw chuck, the four-jaw chuck, the collet, or the faceplate. For round or hexagonal workpieces, three-jaw chuck is used while four-jaw chuck and collet are used for irregular-shaped workpieces.

In boring of steels, vibration of tool and workpiece are the important limiting factor for volume of metal removed and machining efficiency. In boring operations, the length of boring bar is kept long, resulting in vibrations leading to tool failure, poor surface finish, and chatter. The ratio of length to diameter of boring bar is one of the important factors that is responsible for tool vibration. It has been established that boring bars with a high length–diameter ratio tend to chatter.[1] In the industry where metal cutting operations such as turning, milling, boring, and grinding take place, degrading vibrations are a common problem. In internal turning operation, vibration is a pronounced problem, as long and slender boring bars are usually required to perform the internal machining of workpieces. Tool vibration in internal turning frequently has a degrading influence on surface quality, tool life, and production efficiency, and will also result in severe environmental issues such as high noise levels. Boring bar vibrations are usually directly related to the lower order bending modes of the clamped boring bar.[2,3]

The concern today in the manufacturing industry is the vibration induced by metal cutting, for example, turning, milling, and boring operations. Turning operation and especially boring operations are associated with serious vibration-related problems. To reduce the problem of vibration and ensure that the desired shape and tolerance are achieved, extra care must be taken with production planning and in the preparations for the machining of a workpiece. The vibration problem associated with metal cutting thus has considerable influence on important factors such as productivity, production costs, etc. Hence, the need for thorough investigation of the factors that cause vibrations in machining operation is therefore an important step toward solving the problem. In internal turning, the metal-cutting process is carried out in predrilled holes or holes in cast, etc. The dimensions of the workpiece hole generally determine the length and limit the diameter or cross-sectional size of the boring bar.

Usually, a boring bar is long and slender and is thus sensitive to excitation forces introduced by the material deformation process in the turning operation. The boring bar is generally the weakest link in the boring bar–clamping system of the lathe. The boring bar motion may vary with time. This dynamic motion originates from the deformation process of the work material. The motion or vibration of the boring bar influences the result of the machining in general, and the surface finish in particular. Tool life is also likely to be influenced by the resulting vibrations. The tool vibrations during turning are usually denoted 'self-excited chatter' or 'tool

vibration.' Depending on the driving force of the tool vibration, the vibration is generally divided into one of two categories: regenerative chatter and non-regenerative chatter (primary chatter).[4–7] Primary chatter may arise from different physical causes, for example, random excitation of the tool holder's eigen frequencies due to plastic deformation of workpiece material and/or friction between the tool and the cut material, the tendency of the cutting force excitation to change with the cutting speed, and the dynamic effects of the geometry of the cutting tool on the cutting process, etc.[4,7,8] Regenerative chatter is induced by the undulation on the surface of the workpiece which is produced during previous successive cuts.[4,9]

During an internal turning operation, the cutting tool and the boring bar are subjected to a prescribed deformation as a result of the relative motion between the tool and workpiece both in the cutting-speed direction and feed direction. As a response to the prescribed deformation, the tool is subjected to traction and thermal loads on those faces that have interfacial contact with the workpiece or chip. In the metal-cutting process, during which chips are formed, the workpiece material is compressed and subjected to plastic deformation. This results in considerable strain and strain rates in the primary deformation zone. **Figure 1** shows a typical boring operation process.

Also, the dynamic properties of a boring bar installed in a lathe are influenced by the boundary conditions imposed by the clamping of the bar.[2,10] A number of theories concerning the machine tool chatter and the behavior of the dynamic system have been developed explaining tool vibration during turning operations.[4,11–13] In 1946, the principles of the traditional theory of chatter in simple machine-tool systems was worked out by Arnold[11] based on experiments carried out in a rigid lathe, using a stiff workpiece but a flexible tool holder. In this way he was able to investigate chatter under controlled conditions. Later in 1965, Tobias[4] presented an extensive summary of results from various researchers concerning the dynamic behavior of the lathe, the chatter theory, and further

developed the chatter phenomena considering the chip-thickness variation and the phase lag of the undulation of the surface. Also, in the same year, Merritt[12] discussed the stability of structures with n-degrees of freedom, assuming no dynamics in the cutting process; they also proposed a simple stability criterion.

### 1.2.2   Factors Affecting Boring Operation

Like any other machining operations, output results are determined by the cutting conditions such as cutting speed, feed rate, depth of cut (DOC), type of tool, tool geometry, cutting fluid type, and method of application, machining type and materials. Hence, researchers have employed some of these cutting conditions to investigate how they affect the boring operation in terms of surface finish, cutting force, too wear, tool vibration, dimensional accuracy, etc. Akesson et al.[14] investigated the dynamic properties of boring bars concerning different clamping conditions. The experimental setup and subsequent measurements were carried out on a Mazak SUPERQUICKTURN – 250 M computer numerical control (CNC) turning center. The CNC lathe has 18.5 kW spindle power and a maximal machining diameter of 300 mm with 1005 mm between the centers, a maximal spindle speed of 400 revolutions per minute (rpm) and a flexible turret with a tool capacity of 12 as shown in **Figure 2**.

Two different boring bars were used in the experiment. The first boring bar used in the modal analysis was a standard 'non-modified' boring bar, WIDAXS40TPDUNR15F3D6G. The second boring bar used was a modified boring bar, based on the standard WIDAXS40TPDUNR15 boring bar with an accelerometer and an embedded piezo-stack actuator. The accelerometer was mounted 25 mm from the tool tip to measure the vibrations in the cutting-speed direction (y-). This position was as close as possible to the tool tip, but at a sufficient distance to prevent metal-chips from the material removal process from damaging the accelerometer. The standard WIDAXS40TPDUNR15 boring bar was manufactured using material 30CrNiMo8 (AISI4330), which is a heat treatable steel alloy (for high strength). Shaker excitation was used for the experimental modal analysis of the boring bars. The utilized spectrum estimation parameters and excitation signals' properties were determined. A frequency range covering the significant part near the resonance frequencies was selected, i.e., − 100 to − 200 Hz around the resonance peaks. The coherence values for the involved transfer paths at each eigen frequency were greater or equal to 0.996.

A number of different phenomena were observed during the experimental modal analysis of the boring bars for various configurations and setups. For instance, large variations were observed in the first resonance frequencies of the boring bar for different tightening torques of the clamp screws. Also, the order in which the clamp screws were tightened (first from the upper side of the boring bar or first from the underside of the boring bar) had a significant impact on, for example, the fundamental bending resonance frequencies. The results from the experimental modal analysis of the two boring bars demonstrate that the different controlled clamping conditions in the experiments yield different dynamic properties of the
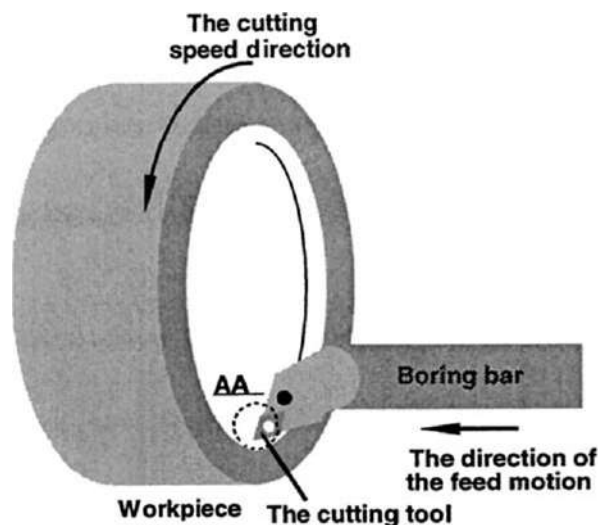
Figure 1   Boring operation.[2]
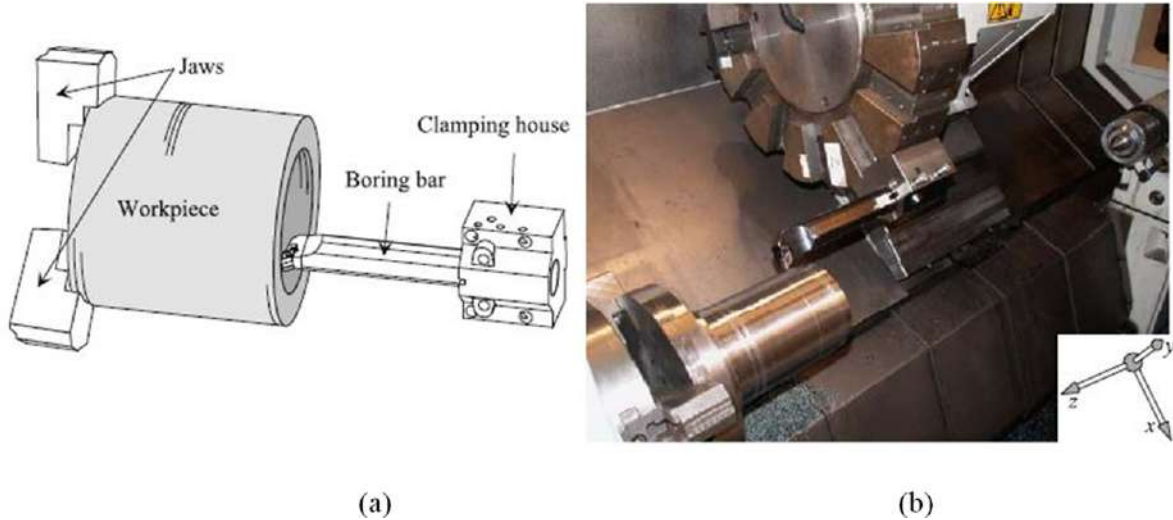
Figure 2   (a) An internal turning setup with a workpiece clamped in a shuck to the left and a boring bar clamped in a clamping housing to the right. (b) The room in the Mazak SUPERQUICKTURN – 250 M computer numerical control lathe where machining is carried out.[14]

clamped boring bars. Hence, the different clamping conditions result in different boundary conditions along the clamped part of the boring bar. It was also established that a boring bar clamped in a standard clamping housing with clamping screws is likely to have a nonlinear dynamic behavior. The standard clamping housing with clamp screws is the likely source of the nonlinear behavior. Multi-span Euler–Bernoulli models of a clamped boring bar incorporating pinned or elastic support boundary conditions approximating the flexibility of the actual screw clamping of the boring bar end inside the clamping housing provide significantly higher correlation with experimental modal analysis results compared to a traditional fixed-free Euler–Bernoulli model.

The fundamental boring bar resonance frequencies decrease with increasing excitation level. However, with regard to the behavior of relative damping as a function of excitation force level; the results from the standard boring bar indicate that the relative damping for the first mode increases with increasing excitation force level, while the relative damping for the second mode decreases with increasing excitation force level. Also, the results from the modified boring bar give an ambiguous indication of the effects on damping properties and the clamp screw tightening torque appears to affect the nonlinear behavior of the boring bar. The investigation shows that the number of clamping screws, the clamping screw diameter sizes, the screw tightening torques, and the order the screws are tightened has a significant influence on a clamped boring bars eigen frequencies and its mode shapes orientation in the cutting speed – cutting depth plane. The results indicated that multi-span Euler–Bernoulli beam models with pinned boundary condition or elastic boundary condition modeling the clamping are preferable as compared to a fixed-free Euler–Bernoulli beam for modeling dynamic properties of a clamped boring bar. It also demonstrated that a standard clamping housing clamping a boring bar with clamping screws imposes nonlinear dynamic boring bar behavior.

Rao et al.[1] evaluated the cutting tool condition monitoring by analyzing surface roughness, workpiece vibration, and

Figure 3   Workpiece.[1]

volume of metal removed for AISI 1040 steel in boring. The experiment was conducted on CNC lathe DX200 model, with tool inserts of DNMG150608 and DNMG150604 having nose radii of 0.8 and 0.4 mm respectively. The metal used in this experiment was AISI1040 with length of 90 mm, outer diameter of 100 mm, and inner diameter of 56 mm as shown in **Figure 3**.

The following sequential procedure was used to carry out the experiment under dry conditions.

1. Each test was started with a fresh cutting edge with one test condition (trials) and machining stopped at the end of each pass. After each pass the DOC was increased by 0.2 mm (fixed DOC was given in each pass) until the tool failed.
2. Vibration signals from the rotating workpiece were measured in the machining process using LDV.
3. After each pass the tool insert was removed and flank wear and crater wear were measured with machine vision system.
4. After each cut the workpiece was also removed and its surface roughness measured on Talysurf.

5. The steps one to four to be continued until the tool failed and beyond that two or three passes performed on the workpiece to observe the behavior of tool wear.
6. A new workpiece and new tool insert were loaded to the machine and the above steps were followed with a new working condition.
7. In each trial, surface roughness, volume of metal removed, and time and amplitude of workpiece vibrations were identified when the tool failed based on flank wear. The above procedure was followed for all the trials and in each trial the cutting parameters were changed as given in the Table 1.

Taguchi, analysis of variance (ANOVA) and regression analysis methods were used to analyze the experimental data to find out the effect and contribution of cutting parameters. According to selected orthogonal array eight experiments (trials) were conducted with two levels of cutting parameters such as workpiece rotational speed, tool insert nose radius, and feed rate. The results show that in each trial of experiment, a strong correlation among the dependent and independent variables was found. A noncontact monitoring system was used with Laser Doppler Vibrometer to observe vibration of workpiece during machining. Tool life was evaluated by analyzing surface roughness, amplitude of workpiece vibration, and volume of metal removed with the help of Taguchi, ANOVA, and regression analysis. The following results were observed during the experiment.

1. Vibration amplitudes of workpiece are found to be increased along with the progression of the tool wear.
2. Nose radius (45.81%) is the significant parameter for affecting the amplitude of workpiece of vibration.
3. Feed rate (55.57%) is the significant parameter for affecting the surface roughness.
4. Feed rate (51.26%) is the significant parameter for affecting the volume of metal removed.

Andren et al.[3] studied the identification of motion of cutting tool vibration in a continuous boring operation – correlation to structural properties. The experimental modal analysis and the operating deflection shape (ODS) analysis were carried out on a Mazak SUPER QUICK TURN – 250 M CNC turning center. It has 18:5 kW spindle power and a maximum machining diameter of 300 mm; with 1007 mm between the center. The cutting operations were performed as an external turning operation using the WIDAX S40TPDUNR15 boring bar. The measurements were divided into two different categories: modal analysis and ODS analysis of the boring bar. In the

Table 1   Test trails for boring[1]

S/N	Speed (m min^{-1})	Feed (mm rev^{-1})	Nose radius (mm)
1	210	0.10	0.8
2	210	0.16	0.8
3	170	0.10	0.8
4	170	0.16	0.8
5	210	0.10	0.4
6	210	0.16	0.4
7	170	0.10	0.4
8	170	0.16	0.4

modal analysis measurement the following equipment were used: (1) 14 PCB 333A32 accelerometers, (2) OSC audio power amplifier, USA 850, (3) Ling Dynamic Systems shaker V201, (4) Bruel and Kjær 8001 impedance head, (5) Bruel and Kjær NEXUS conditioning amplifier 2692, (6) HP VXI E1432 front–end data acquisition unit, and (7) PC with IDEAS Master Series version 6. The ODS data were collected using less sensitive accelerometers than those used in the modal analysis measurement. For the ODS analysis, the boring bar vibration was measured during a continuous cutting operation and data were collected using the following measuring equipment: (1) 14 PCBU353B11 accelerometers, (2) HP VXI E1432 front–end data acquisition unit, and (3) PC with IDEAS Master Series version 6.

The experimental modal analysis of the boring bar with modified clamping resulted in two identified modes. The first mode in the cutting depth direction had a resonance frequency of 570 Hz; and a relative (viscous) damping of 1.85%. The second mode in the cutting-speed direction had a resonance frequency of 595 Hz and a damping of 0.84%. The damping of the first mode was noted to be slightly larger than prior to the modification of the clamping. The two modes were well separated as defined by the cross MAC value and the synthesized frequency response functions corresponded well with the measured functions. From the ODS results, it was apparent that vibrations of the boring bar were dominating in the cutting-speed direction during a continuous cutting operation. The deformation pattern of the boring bar was according to the ODS measurement dominating in the cutting-speed direction at both resonance peaks. The ODS resulted in eigen frequencies at a somewhat lower frequencies compared with the modal analysis.

Saindane et al.[15] investigated the effect of vibration damping in boring operation using passive damper. Boring bar of 16 mm × 16 mm cross section and 200 mm long of WIDAX make was used. The boring operations were carried out on a lathe machine as shown in Figure 4 using EN9 as workpiece material. The workpiece was mounted on the lathe using a four-jaw chuck. The machining parameters were selected based on the manufacturers recommendations and were changed according to the proposed conditions. Also the cutting speed, length of passive damper on boring bar, and overhang length were varied as shown in Table 2 and experiments were conducted to analyze the effect of vibration on deflection of boring bar.

The boring operation was carried out for 51 mm internal diameter using passive dampers of nylon and polyurethane. Fast Fourier transform (FFT) analyzer and accelerometer were used to obtain various results for the experiments and the deflections were measured in terms of acceleration by accelerometer as shown in Table 3.

It was observed that the proposed method was an innovative to reduce the deflection of the boring bar in boring operation. The results proved the passive damping technique has vast potential in the reduction of deflection and depend on the DOC. Passive dampers are also relatively cheaper than other damped boring bars.

Khatake and Nitnaware[16] studied the mitigation of vibration using passive damper in machining. The study involved the use of particle damper, which is a passive damping concept

Figure 4 Experimental set up of boring bar with passive damper and accelerometer.[15]

Table 2   Experimental conditions[15]

S/No	Cutting speed (rpm)	Feed rate (mm rev^{-1})	Depth of cut (mm)	Overhanging of the boring bar (mm)	Material used for damping	Percentage of overhang damped	Length of passive damper
1	100	0.02	1	100	Nylon	3	30
2	100	0.02	1	120	PU	6	72
3	100	0.04	2	100	Nylon	6	60
4	100	0.02	2	120	PU	3	36
5	120	0.02	2	100	PU	3	30
6	120	0.04	2	120	Nylon	6	72
7	120	0.04	1	100	PU	6	60
8	120	0.04	1	120	Nylon	3	36

Table 3   Experimental results[15]

S/No	Without damper (mm)	With damper of polyurethane ($\mu m\,s^{-2}$)	With damper of nylon ($\mu m\,s^{-2}$)
1	28	22	25
2	50	40	30
3	40	50	30
4	25	28	40
5	24	25	23
6	40	30	20
7	25	22	18
8	48	35	20

that uses metal or ceramic particles or powders of small size that are placed inside cavities within or attached to the vibrating structures. Metal particles of high density such as lead or tungsten steel are the most common materials for better damping performance. In contrast to viscoelastic materials which dissipate the stored elastic energy particle damping treatment focuses on energy dissipation in a combination of collision, friction, and shear damping. It involves the potential of energy absorption and dissipation through momentum exchange between moving particles and vibrating walls,

friction, impact restitution, and shear deformations. It is an attractive alternative in passive damping due to its conceptual simplicity, potential effectiveness over broad frequency range, temperature, and degradation insensitivity and very low cost. The principle adopted in the study was to enhance the damping capability, minimizing the loss in static stiffness through implementation of passive damper.

Boring bar of 20 mm × 20 mm cross section and 200 mm long of WIDAX make was used on EN9 workpiece material. The boring operations were carried out on CNC center lathe. The workpiece was mounted using a pneumatic chuck. The machining parameters such as feed rate (0.09 mm min^{-1}), DOC (0.6 mm^{-1}), clamping pressure (10 bar), etc., were selected based on the manufacturers recommendations and were kept constant for all the samples used. Only the cutting speed, passive damper position on boring bar, and overhang length were changed as shown in **Table 4**. Boring was carried out for 110 mm internal diameter using newly designed tool and conventional tool. The evaluation criteria were the dynamic characteristics, frequency, and damping ratio, of the machining system, as well as the surface roughness of the machined workpieces.

Table 5 shows the results obtained for cutting speed of 210 rpm, DOC of 0.6 mm and feed rate of 0.09 mm min^{-1}.

Table 4   Experimental conditions[16]

Boring tool	BT1	BT2	
Overhang length L (mm)	30	60	90
Position of passive damper	Vertical	Horizontal	
Cutting speed (rpm)	70	140	210

Table 5   Experimental results[16]

S/N	Overhang length of boring bar (mm)	Surface finish (μm) without passive damper	Surface finish (μm) with passive damper	
			Vertical	Horizontal
1	30	2.63	2.41	2.63
2	60	2.59	2.51	1.46
3	90	2.80	3.19	3.25

The result shows that the results prove the passive damping technique has vast potential in the reduction of tool chatter. It is therefore concluded that passive damping has a good effect in improving surface finish in boring operation and significant improvement was observed between the results of surface finish obtained using boring bar without passive damper and boring bar with passive damper.

Kadu et al.[17] formulated a mathematical model for the investigation of tool wears in boring machining operation on cast iron using carbide and cubic boron nitride tools. The process of formulation of mathematical model for optimizing the tool life in casting machining operation and its analysis in this study involved two levels for each independent parameter taken. In tool life optimization process, the objective of the experiment was used to gather information through experimentation for formulation of mathematical model for cast iron machining operation. During cast iron machining operations, the measurement of tool life, surface finish, bore size variation, operation time, and spindle load was measured using meter scale, surface finish tester, digital dia. test plug gauges, digital stopwatch, and current in percentage amp. Energy and time were measured using energy meter and stopwatch respectively. Pilot experiments were performed to select test envelope and test points of process parameters for experimental design. These process parameters as shown in **Table 6** were used in experimental design for the investigation of process parameters like cutting speed, nose radius, length, diameter, and material of the cutting tool, cutting fluid pressure, and concentration and DOC for casting machining operation. The observed values for tool life, surface finish, bore size variation, operation time, and spindle load were recorded for formulation of mathematical model. In casting machining operation observations were taken out at two levels for each independent parameter.

One hundred and twenty-eight experiments were designed on the basis of sequential classical experimental design technique that has been generally proposed for engineering applications.[18] The basic classical plan consists of holding all but one of the independent variables constant and changing this one variable over its range. The main objective of the experiments consists of studying the relationship between 09 independent process parameters with the 05 dependent responses for tool life optimization. Simultaneous changing of all 09 independent parameters was cumbersome and confusing. Hence all 09 independent process parameters were reduced by dimensional analysis. Buckingham's π theorem was adapted to develop dimensionless π terms for reduction of process parameters. This approach helps to better understand how the change in the levels of any one process parameter of a π terms affects 05 dependant responses for cast iron boring machining operation. Out of five response/dependant variables two dependant variables cutting time and surface roughness were evaluated. A combination of the levels of parameters, which lead to maximum, minimum, and optimum response, can also be located through this approach. Regression equation models of tool life were optimized by mini–max principle.[19]

The authors observed that (1) the dimensionless π term have provided the idea about combined effect of process parameters in that π terms. A simple change in one process parameter in the group helped the manufacturer to maintain the required torque (To) and surface roughness (Ra) values so that to get increased tool life. (2) The mathematical models developed with dimensional analysis for different combinations of parameters for cutting speed, nose radius, length, diameter, and material of the cutting tool, cutting fluid pressure and concentration, and DOC can be effectively utilized for cast iron boring machining operations. (3) The computed selection of cast iron boring machining operation parameters by dimensional analysis provides effective guidelines to the manufacturing engineers so that they can minimize To and Ra for higher performances. (4) The models have been formulated mathematically for the Indian conditions. The comparison of values of dependent term obtained from experimental data, mathematical model, and ANN. From the values of percentage errors, it seems that the mathematical models can be successfully used for the computation of dependent terms for a given set of independent terms. Indian industries can use the data for calculation cutting time, tool life, surface roughness, bore size variation, and spindle load estimation for cast iron boring machining operations.

Badadhe et al.[20] conducted an experiment to optimize the cutting parameters in boring operation. Four parameters, i.e., spindle speed, feed, DOC, and length–diameter (L/D) ratio of boring bar were considered as input variables. **Tables 7** and **8** show the input factors and levels used in the experimental design and experimental matrix of 3^4 orthogonal array respectively. Total nine runs (L$_9$) were conducted during one trial. Trials were repeated to check the consistency in the output. Cutting trials were conducted on Kirloskar make (Enterprise-500) center lathe machine. AISI 1041 carbon steel cylinders with 100 mm outside diameter, 85 mm inside diameter, and 75 mm length were used as workpieces.

Standard boring bars with Widax tool holder S25TPCLNR12F3, S20SSCLCR09T3, and S16QSCLCR09T3 along with cemented carbide inserts having radius 1.2 mm were used for metal cutting. Surface finish was measured off-line by using HOMMELWERKE TURBO RAUHEIT V 6.14, Swiss make surface recorder having 0.8 mm cut-off and 4.8 mm sample length. The ANOVA was carried out to find the significant factors and their individual contribution in the response function, i.e., surface roughness.

Table 6   Test envelope and test points for cast iron boring machining operation[17]

Pi term	Equation	Test envelope	Test points	Independent variable with its own range
Π_1	Tool geometry parameters: $\left(\frac{LD_{pc}NR}{D^3}\right)$	(0.000162–0.0012096)	0.000162 0.000227 0.00025 0.00028 0.000324 0.00035 0.000392 0.000432 0.000454 0.0005 0.00056 0.000605 0.0007 0.000784 0.000864 0.00121	L, mm − 175,270 Dpc, mm − 0.5,0.7 NR, mm − 0.4,0.8 D, mm− 50,60
Π_2	Cutting speed: $\left(\frac{Vc}{(Dg)^{0.5}}\right)$	(0.46923–0.706782)	0.469237 0.514024 0.645201 0.706782	g, mm sec^{-2} − 9810 D, mm − 50,60 Vc-mm sec^{-2} − 360,495
Π_3	Coolant concentration and pressure: $\left(\frac{g.Cc}{PcD^5}\right)$	(4.21E-06–1.88E-05)	4.21E-06 5.05E-06 6.31E-06 7.57E-06 1.05E-05 1.26E-05 1.57E-05 1.88E-05	g, mm sec^{-2} − 9810 Pc-N mm^{-2} − 10,15 D,mm-50,60, Cc N mm^{-3} − 5, 6
Π_4	Material Hardness: $\left(\frac{Hm}{Pc}\right)$	(1831.2–4414.5)	1831.2 2746.8 2943 4414.5	Hm, N mm^{-2} Tn Carbide − 27468 cubic boron nitride-44145 Pc, N mm^{-2}–10,15

Table 7   Experimental levels[20]

S/No	Control variables	Level 1	Level 2	Level 3
A	Spindle speed (rpm)	54	140	224
B	Feed rate (mm rev^{-1})	0.045	0.36	0.676
C	Depth of cut (mm)	0.5	0.75	1
D	L/D ratio for boring bar (mm)	4	5	6.25

Table 8   Basic Taguchi L$_9$ (3^4) orthogonal array[20]

Run	A	B	C	D
1	1	1	1	1
2	1	2	2	2
3	1	3	3	3
4	2	1	2	3
5	2	2	3	1
6	2	3	1	2
7	3	1	3	2
8	3	2	1	3
9	3	3	2	1

The averages of surface roughness values obtained during each trial (Ra_1 and Ra_2) and the Signal-to-Noise (S/N) ratio calculated for the criteria of lower-the-better are shown in **Table 9**.

The optimal values of the input factors A, B, C, and D were obtained from S/N ratio as shown in **Table 10** using the lower the better characteristic. The S/N ratio for spindle speed is higher at level 3, similarly for others the values are feed 1, DOC 2, and L/D ratio 1. Hence the optimal combination of control factors were given as 3-1-2-1 and this is represented on the plot of **Figure 5**.

ANOVA was carried out to check the significant contribution of each input factor in response function. **Table 11** shows the results of the ANOVA for surface roughness. It can be observed from the ANOVA result, that the parameters A, B, and D are having significant contribution of 28%, 30%, and 36% respectively in the response function (Ra) whereas the parameter C has relatively less contribution and thus is of less importance.

The study shows that the control factors had varying effects on the response variable and the use of the Taguchi parameter design technique was considered successful as an efficient method to optimize machining parameters in a boring operation.

Table 9   Experimental results for surface roughness and calculated value for S/N ratio[20]

Run	A	B	C	D	Ra	S/N ratio
1	54	0.045	0.5	4	3.63	−11.1981
2	54	0.36	0.75	5	11.30	−21.0616
3	54	0.676	1	6.25	13.70	−22.7344
4	140	0.045	0.5	6.25	5.97	−15.5195
5	140	0.36	0.75	4	6.82	−16.6757
6	140	0.676	1	5	10.20	−20.1720
7	224	0.045	0.5	5	4.59	−13.2363
8	224	0.36	0.75	6.25	7.66	−17.6846
9	224	0.676	1	4	2.99	−9.5134

Table 10   Calculated mean S/N ratios[20]

Level	A	B	C	D
1	−18.33	−13.32	−16.35	−12.46
2	−17.46	−18.47	−15.36	−18.16
3	−13.48	−17.47	−17.55	−18.65
Delta	4.85	5.16	2.18	6.18
Higher S/N ratio	3	1	2	1

Moetakef-Imani and Yussefian[21] studied the dynamic simulation of boring process. The study involved the use of a boring bar with 20 mm diameter and 140 mm length ($L/D=7$) to implement the machining tests. Carbide inserts with 0.4 mm nose radius and flat rake face were used to machine the aluminum 6061 tubes. The dynamic properties of boring bar and geometrical properties of the cutting tool are presented in **Tables 12** and **13** respectively.

The cutting speed, feed rate, and radial DOC were in the range of 70–110 m min^{-1}, 0.08–0.24 mm rev^{-1}, and 0.2–4 mm respectively. Cutting force components were measured in three orthogonal directions by a KISTLER9255b dynamometer. The dynamic simulation program was also implemented for every corresponding machining experiment. For the sake of comparison between the experimental measurements and numerical simulations, two different cutting tests were presented. The cutting conditions for these two cutting experiments are shown in **Table 14**.

The DOC was set to 0.5 and 4 mm for tests A and B respectively. All other conditions for these tests are equal. In order to validate the proposed method, 30 boring experiments were conducted. **Figure 6** shows the algorithm for dynamic simulation of boring process.

Measured and predicted cutting force components for boring with machining conditions of test A are depicted in **Figure 7**. When the tool first engaged the cut, it undergoes transient vibrations. But after several revolutions, the cutting process becomes stable and the tool continues to vibrate periodically with relatively constant amplitude.

So the condition of test A was stable and chatter-free cutting machining operation. The simulated peak frequency occurred at 672 Hz with a deviation of 12.94% above the measured value of 594 Hz. It was observed that the deviation resulted from the over estimation of the eigen frequencies by the Euler–Bernoulli beam equation. When the results of cutting force components measured by a dynamometer was compared with the simulated results by the proposed algorithm. The measured values of the cutting force components in x, y, and z direction were predicted by 9%, 2%, and 12% errors in magnitude. This amount of error was consistent with the validity interval of $\pm 10\%$ for the cutting force computation[22] which could be due to the cutting force coefficient computations.

Experimental and simulated cutting force components in time domain for the condition of test B are shown in **Figure 8**. It was observed from the measured data that the machining process was unstable with chattering frequency around 573 Hz. In case of chatter, measured force components oscillate randomly and grow rapidly to large amplitudes. It could be seen from **Figure 8** that the simulated results had also predicted the incidence of chatter vibrations. Although the model was capable of truly predicting the chatter occurrence for the conditions of test B, the variation of simulated and measured cutting force amplitudes is increased.

This is due to the fact that the measured cutting force components have been amplified by chatter frequency.[23] As a consequence of high-vibration amplitudes, the actual geometrical angles of the cutting tool will change from their nominal values. It is well known that the variation of cutting tool angles will affect the cutting force components significantly.[22,24] The high-reciprocating velocity of the tool tip makes the cutting process be accompanied with the plunging of the tool in to the workpiece. The high acceleration of the tool increases the effect of the tool inertia forces on dynamometer measurements. All of these will make the prediction of dynamic characteristic of the process under chatter vibration almost impossible. However, for any dynamic model the correct prediction of chatter onset is enough since no practical machining operation will be carried out under chatter conditions.

The researchers were able to develop a model to simulate the dynamics of boring process. The developed model relies on the novel algorithms of geometrical modeling. In contrast to the previous models that were only able to predict the stability region, this model computes the dynamic cutting force components and frequencies in stable boring operation. The performed cutting experiments have shown that the cutting force components and the vibration frequencies in chatter-free dynamic boring operation could be predicted within $\pm 15\%$ error margin. The model is valid for both finishing (DOC<r) and roughing (DOC>r) boring processes. The model is also able to predict the chatter onset in boring
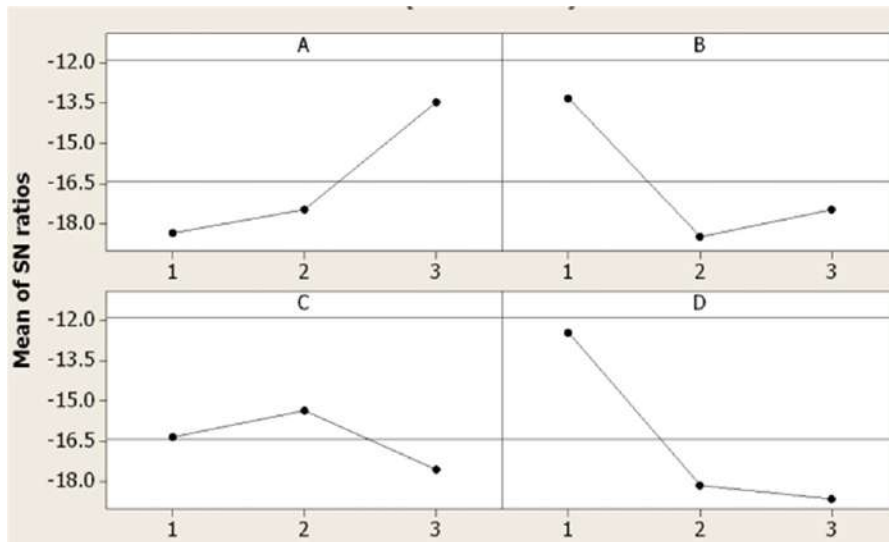
Figure 5   Plots for mean S/N ratios for A, B, C, and D.[20]

Table 11   Results of the ANOVA for surface roughness[20]

Source of variation	df	Sum of squares	Mean square	F-ratio	Contribution (%)
Spindle speed (A)	2	60.30	30.15	59.66	27.65
Feed rate (B)	2	66.02	33.01	65.33	30.28
Depth of cut (C)	2	8.48	4.24	8.39	3.89
L/D ratio (D)	2	78.65	39.32	77.82	36.07
Error	9				
Total	17				

Table 12   Dynamic properties of boring bar[21]

Parameter	L_e (m)	L (m)	ξ_y	w_{1y} (Hz)
Value	0.1535	0.14	0.025	620

Table 13   Geometrical specifications of the cutting tool[21]

Parameter	L (m)	r (mm)	α_s (deg)	α_b (deg)	c_s (deg)	c_e (deg)
Value	0.14	0.4	− 5	0	− 3	32

Table 14   Geometrical specifications of the cutting tools for tests A and B[21]

Parameter	Depth of cut (mm)	c (mm rev^{-1})	V (m min^{-1})	DO (mm)	Result
Test A	0.5	0.14	95	30.5	Stable
Test B	4	0.14	95	30.5	Chatter

Figure 6   Algorithm for dynamic simulation of boring process.[21]

operation. Due to the nonlinear geometry of the edge, the influence of DOC and feed rate is interrelated and should not be separately investigated. The instantaneous chip load is computed to incorporate the effect of DOC and feed rate. The influence of geometrical 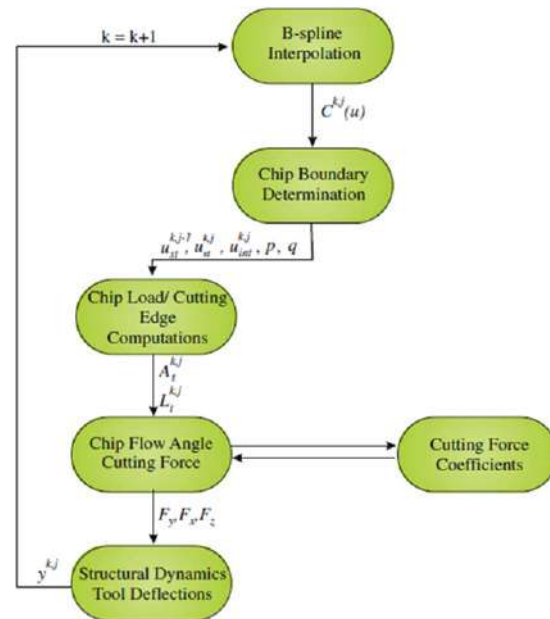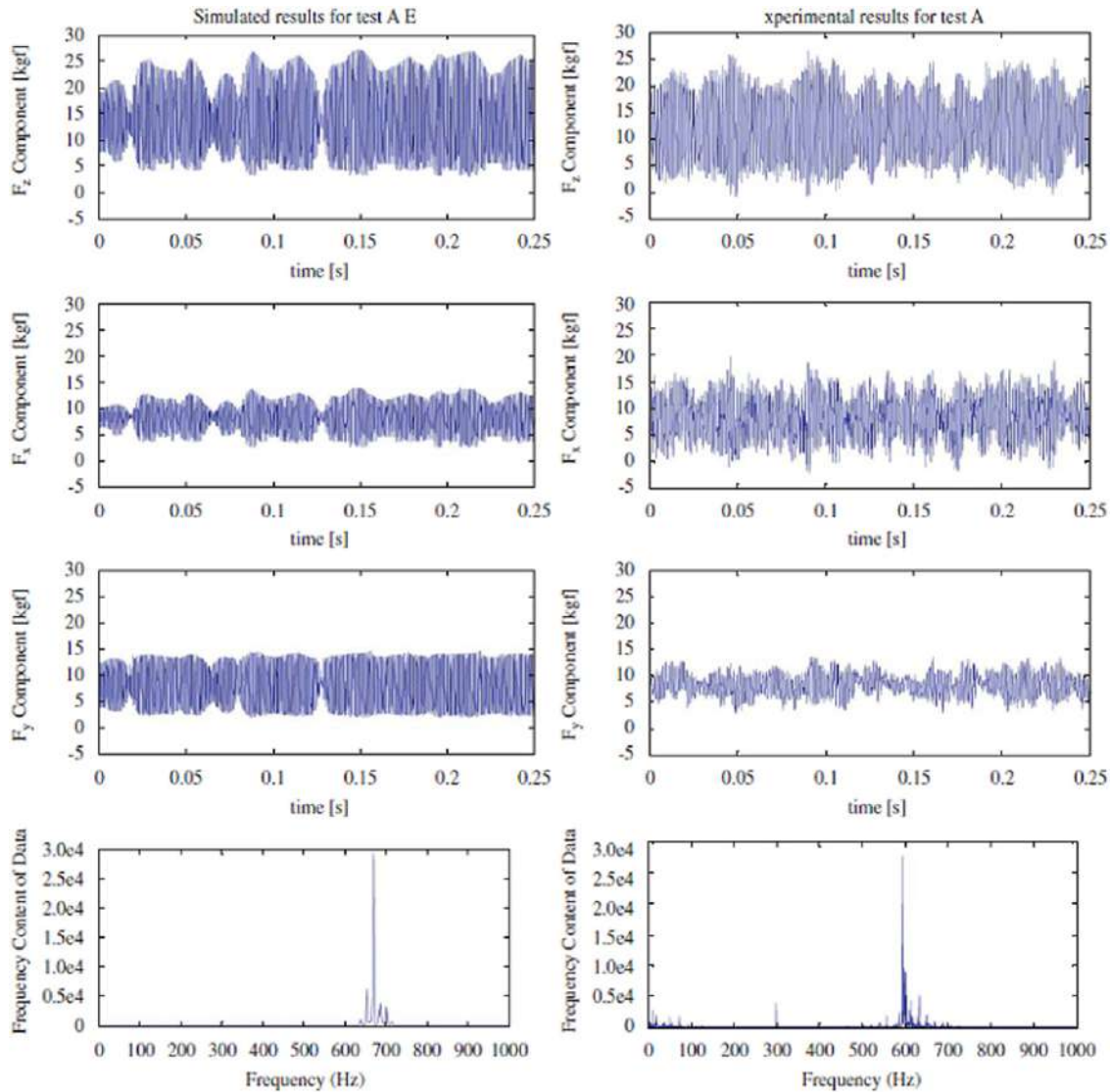properties (like tool angles and nose radius) as well as structural and process parameters could be investigated using this model. The stability and efficiency of the process depends on the combined effect of all these

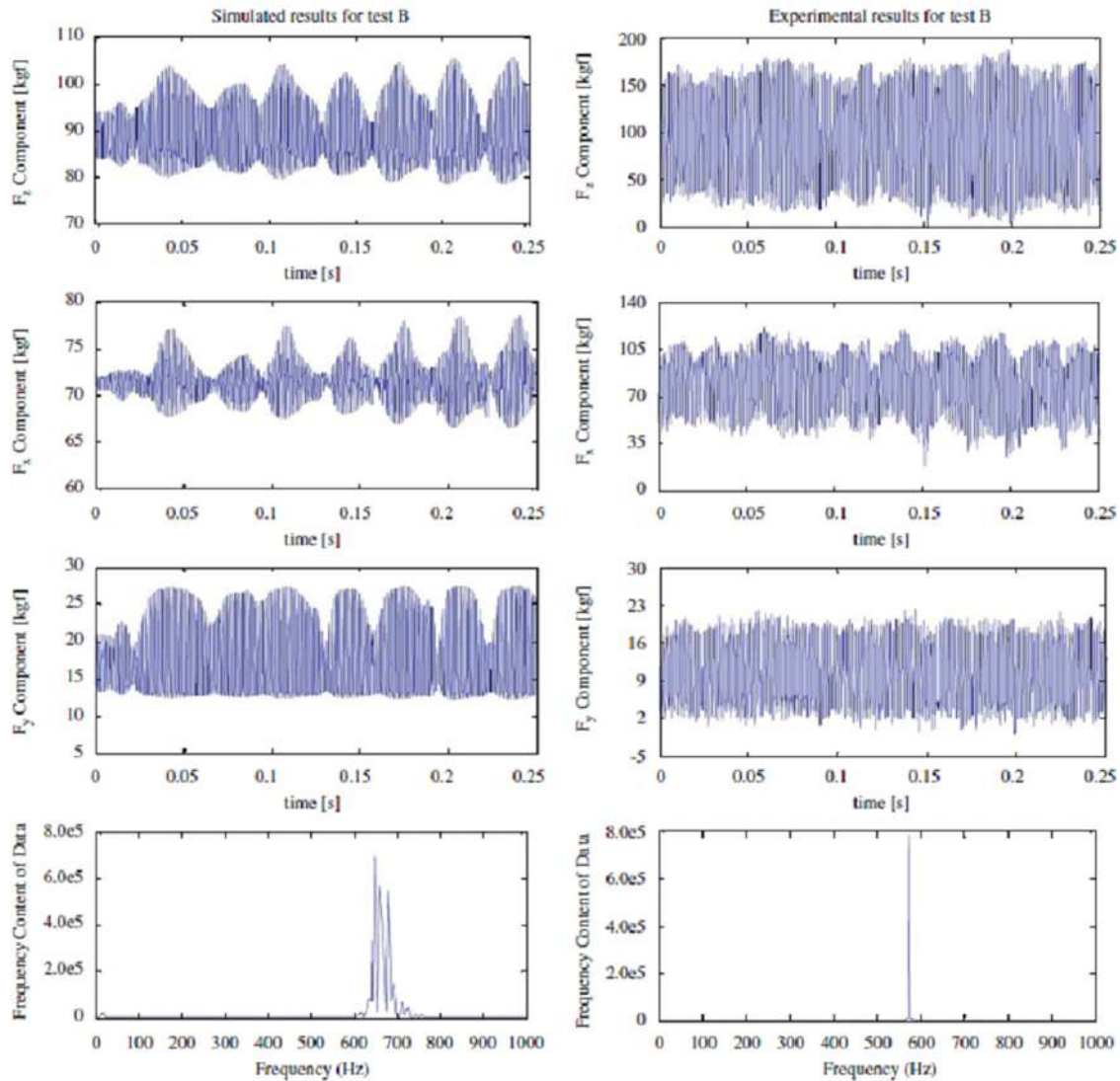**Figure 7**   Experimental and simulated cutting force values for test A.[21]

parameters. Hence, the proposed model provides a better understanding of a certain boring process.

Byung-Kwon Min et al.[25] studied the use of smart boring tool for process control. The experiment involved the evaluation of the performance of the tool tip servo under real machine tool operating conditions, cutting tests were performed using a stationary Smart Tool boring bar and rotating workpiece. For the cutting test, an aluminum workpiece made from thick wall tube with a 180 mm diameter hole was used. The Smart Tool boring bar was attached to a turning machine tool post and the workpiece was attached to spindle. The tool tip position measurement was recorded to the memory of the controller computer. The spindle speed was 510 rpm corresponding to a cutting speed of 4.8 m s^{-1}. The feed rate was 0.21 mm rev^{-1}. Step response and sine wave tracking were conducted. The purpose of the step response experiment was to determine what tolerances could be maintained in the position of the tool tip relative to the fixture, as well as the effects of cutting on the transient response of the tool tip servo.

The purpose of the sine wave tracking experiment was to verify the ability of the system to follow sinusoidal references during cutting. This is similar to the objective of isolating the tool tip motion from boring bar vibration. The model parameters and monitoring variables for the experiments are shown in Tables 15 and 16.

Figure 9 illustrates the geometry of finish boring process. As can be seen, if the center of the pre-boring hole and the finish boring tool position are offset due to fixture misalignments, the DOC of the boring process becomes a periodic function that is repeated with every revolution of the spindle.

Tool breakage also results in the deviation of the cutting force from the normal cutting force generated by the boring process. Cutting force is a monotonic function of the DOC and feed rate.[26] Consequently, if the feed is maintained constantly and if the cutting force is accurately measured, the geometric profile of the cutting surface can be estimated from the force data. Cutting tool insert breakage can be monitored in a cutting force changes. For a boring process, the radial direction

Figure 8   Experimental and simulated cutting force values for test B.[21]

component of the cutting force dramatically increases immediately after tool fracture or chipping.[27] Considering the small cutting force generated by finishing process, an excessive rise in the radial cutting force generally indicates finish tool breakage, if the force is bigger than that observed in workpiece misalignment error which will be detailed in the rest of this section.

Based on above observation, the monitoring of fixture misalignment and tool breakage of the Smart Tool boring process can be carried out with force pattern recognition. The radial cutting force estimation described in the previous section has been considered as a method for the monitoring of the Smart Tool boring process. The cutting force estimated by Smart Tool during a single rotation is compared with the radial cutting force measured by a tool dynamometer. The cutting force estimated by Smart Tool during a single rotation is compared with the radial cutting force measured by a tool dynamometer in a polar plot in **Figure 10(a)**. Cutting speed was 2.0 m s^{-1} and feed rate was 0.083 mm per revolution.

A random cutting profile was used to evaluate dynamic performance of the estimator. The difference between the Smart Tool estimation and the tool dynamometer measurement was less than 10% of the cutting force and, thus, the cutting force based on disturbance estimation could be used to detect both the dynamic and the static cutting forces.

Figure 10(b) shows the polar plot of cutting force during a normal boring process operation. **Figures 10(c)** and **10(d)** show the case of workpiece misalignment error and the event of tool breakage respectively. Cutting condition of 2 m s^{-1} cutting speed and 0.083 mm per revolution federate was used for all experimental data. 0.25 mm DOC is used for normal cutting and 0.25 mm desired DOC with 1.27 mm offset was used for misalignment experiment. For the tool breakage experiments, inserts with a 2.0 mm notch was used to expedite breakage. For the normal operation, as can been in **Figure 10(b)**, the cutting force has not deviated more than 10 N from its mean value of 25.96 N and the center of the force plot is close to the center of the graph. The response from misaligned cutting

Table 15   Model parameters[25]

Variable	Value
Piezoelectric actuator	
Young's modulus Y_{33}^E (Pa)	4.8×10^{10}
Strain constant d_{33} (m V^{-1})	5.5×10^{-8}
Maximum voltage V_{max} (V)	100
Density m_p (kg m^{-3})	7500
Maximum current I_{max} (A)	2.0
Area A_p (m^2)	1.0×10^{-4}
Length l_p (m)	0.4
Tool tip translation mechanism	
Width T(m)	0.025
Mass M_m (kg)	0.15
Length l (m)	0.016
Damping b_m (N s/m)	0.025
Length Dl (m)	0.01
Young's modulus E_t (Pa)	2×10^{11}
Boring bar	
Moment of inertia I (m^2 kg)	7.1×10^{-7}
Young's modulus E_b (Pa)	2×10^{11}
Ultimate strength S_{ut} (N)	1.4×10^{11}
Damping b_b (N s m^{-1})	0.013
Yield strength S_e (N)	3.4×10^{10}

Table 16   Monitoring variables[25]

Process status	a	b	R (129.80)	r (5.19)	θ
Normal	1.08	0.50	25.96	1.19	24.95
Workpiece misalignment	30.79	−29.17	24.79	42.58	−43.44
Tool breakage	5.09	3.34	150.93	6.78	29.48
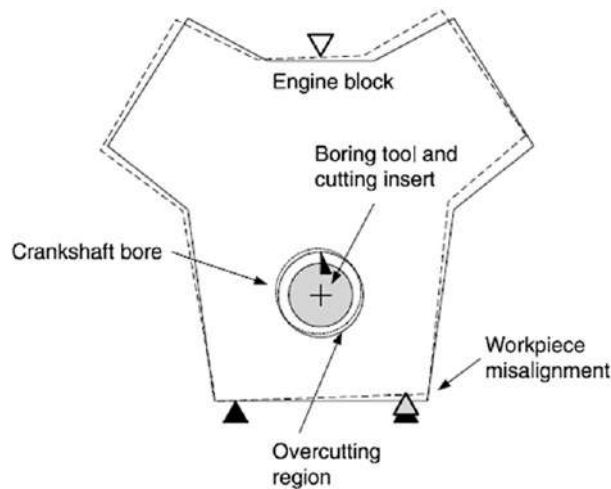
**Figure 9**   Nonuniform depth of cut due to workpiece misalignment error.[25]

plotted in **Figure 10(c)** also shows regular cutting force, but the center of the force plot is shifted from the graph center. The small partial circle in the plot is due to the negative reaction force of the tool when the cutting insert lost the contact with workpiece. The tool breakage recorded in **Figure 10(d)** shows the chaotic behavior of the cutting force with huge force value. As can be seen the plots in **Figure 8**, it is obvious that the different process failures have different force patterns. Therefore, if the difference between the force patterns can be specified quantitatively, monitoring of these failures is possible.

In this experiment, the R and r values calculated from 10 most recent revolutions are used. The R is equal to mean value cutting force. Therefore, regardless of existence of workpiece misalignment error, the excessive R value bigger than critical value is due to tool breakage. The critical cutting force of the tool breakage must be determined by experiment. In this experiment, it is set to 129.80 N which is 500% of measured cutting force, 25.96 N, from normal operation plotted in **Figure 10(b)**. As far as the mean cutting force R is smaller than critical value, the bigger r value indicates workpiece misalignment error. The threshold of r value is also determined by experiment. In the experiment, it is set to 5.19 N which is 20% of normal operation cutting force. This also means threshold of the offset is approximately 20% DOC, even though that is not exact number due to nonlinear relation between cutting force and DOC. From a and b values, which are x and y-directional components of the radial cutting force, the misalignment direction of the hole can be found. The a, b, R, r, and direction of least square center.

The authors were able to develop a mechatronic metal cutting tool to improve the accuracy and flexibility of line boring machining in the automotive industry. Laser position sensors and piezoelectric actuator were integrated into the rotating body of the boring tool, and to compensate the boring bar droop and effects of cutting forces, a fast tool servo utilizing feedback control of the boring tool insert position was designed and embedded in the rotating tool assembly. In addition to position control, a self-monitoring algorithm that utilizes disturbance estimator was put together in the controller. Self-monitoring capability is an important feature in automated machine tool systems and it is more critical when sophisticated mechatronics is used to control the process. This chapter has proposed a tool monitoring method that utilizes the process information and estimated cutting force during tool tip servo control. A new measurement technique of the cutting force based on disturbance estimation was developed and integrated into a sensorized boring tool. The proposed cutting process monitoring method was effective to detect tool failure as well as process failure due to workpiece misalignment errors which occurred in the boring process. The force measurement by the proposed method matches well with the conventional force measurement using a tool dynamometer. The developed accurate cutting force estimation method is not only useful for process failure monitoring, but it is also useful as a substitute for tool dynamometers, especially in cases where the tool dynamometer is difficult to be placed, such as in a rotating tool tip.

Kanase Sandip et al.[28] conducted an experiment on the improvement of surface roughness (Ra) value of boring operation using passive damper. The workpiece was mounted using a pneumatic chuck in CNC turning center and the clamping pressure was set at 10 bars. The machining parameters like feed, DOC, clamping pressure, etc., were selected based on the manufacturers recommendations and were kept
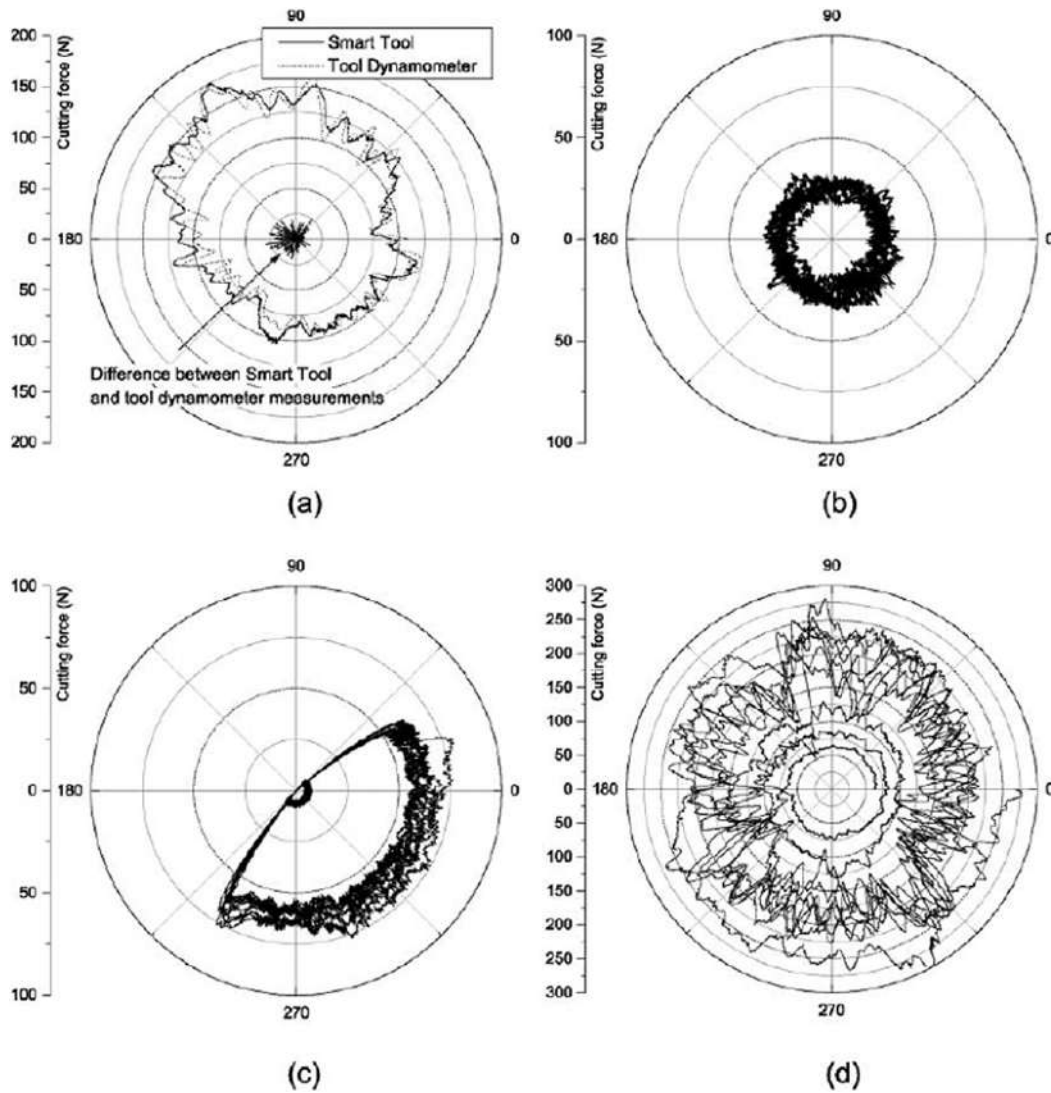
Figure 10   Cutting force measured at Smart Tool. Depth of cut 0.25 mm; feed rate 0.083 mm rev^{-1}; cutting speed 2 m s^{-1}. (a) Comparison with tool dynamometer measurement, (b) normal cutting, (c) workpiece misaligned (tool offset 1.27 mm), and (d) tool breakage.[25]

Table 17   Experimental parameters[28]

Boring tool	BT_A	BT_B	
Overhang length L (mm)	40	80	120
Impact damper position	Vertical	Horizontal	
Clearance CL (mm)	0.4		
Spindle rotation N (rpm)	80	160	240
Feed rate S (mm min^{-1})	0.9		
Depth of cut t (mm)	0.6		

Figure 11   Sample workpiece.[28]

constant for all the samples used. Only the cutting speed, passive damper position on boring bar, and overhang length was changed. The recommended cutting speed, feed, DOC, etc., are shown in **Table 17**. Boring was carried out for 105 mm internal diameter as shown in **Figure 11**.

Twenty five numbers of experiments were conducted to analyze the effect of vibration on surface finish. Boring bar of 20 mm × 20 mm cross section and 200 mm long of WIDAX

make was used. The boring operations were conducted on CNC turning center of ACE make using EN9 workpiece material. A Mitutoyo SJ-201P apparatus was used to determine the surface roughness of the bored surface. **Tables 18–21** show the results obtained for all the experiments conducted under different conditions.

Table 18 Surface roughness without passive damper (cutting speed 240 rpm, doc 0.6 mm and feed rate 0.09 mm min^{-1})[28]

S/No	Test A	Overhang length (mm)	Response (surface roughness, R_a)		
			1	2	3
1	3	40	2.72	2.72	2.73
2	2	80	2.37	2.47	2.69
3	5	120	2.82	2.90	2.60

The results proved the passive damping technique has vast potential in the reduction of tool chatter. Also the suppression in tool chatter by using impact damper boring bars was very significant. Boring bars with impact damping are also relatively cheaper than other damped boring bars. It is therefore concluded that impact damping has a good effect in improving surface finish in boring operation.

Pardeep Kumar et al.[29] conducted an experiment to analysis and optimized the parameters that affect bore deviation (BD) in boring process. A systematic method as outline in the form of flow chat as shown in **Figure 12** was used to optimize the cutting parameters to achieve minimum BD of the Crankcase made up of grade FG 260 of IS: 210–1978.

Randomization of the run order and analysis sequences was carried out according to the run order by Design Expert software 9.0. Full factorial design of three factors with two having three levels and one factor having two levels which consist of 18 runs were adopted. The overall experimental results corresponding to each run generated by the software are shown in **Table 22**. The machining response that was analyzed was BD. All data obtained was then used as input to the Design Expert software 9.0 for further analysis, according to steps outline for full factorial with optimal design.

Design Expert software was used to analyze the results obtained in order to identify the significant factors and interactions between the factors under studied. ANOVA provides information of analysis of variance and case statistics for further interpretation as shown in **Table 23**. Normal probability plot, main effect plot, and interaction plot for the dependent parameters that significantly affect the response were obtained to show the reliability of the results obtained from the experiment.

From the experiment, it has been observed that the existing parameters for finish tappet bore was cutting speed (137 m min^{-1}), feed rate (0.1 mm rev^{-1}), and cutting allowance (0.5 mm^{-1}), whereas for the same dimensions the optimum cutting parameters was cutting speed (160 m min^{-1}), feed rate (0.3 mm rev^{-1}), and cutting allowance (0.3 mm^{-1}). Further, on comparing the values of BD of existing and optimum parameters, the BD was 0.021 mm when the experiments were performed with existing cutting parameters whereas BD obtained with optimum parameters was about 0.015 mm. Therefore there was an approximately 40% of reduction in BD by employing the optimum parameters.

1.2.3 Application of Boring Process in the Building of Tunnel

Boring process is not only restricted to workshop, in fact, it has been applied in the building of tunnels for transportation purpose. Since the need for infrastructure to handle the intercity transportation of people and goods has steadily increased. The construction of such facilities often requires the excavation of long, deep tunnel such as the base tunnels of the Alptransit Project in Switzerland,[30] the Brenner Base tunnel between Austria and Italy,[31] the Lyon-Turin tunnel between France and Italy,[32] or the Gibraltar Strait tunnel between Spain and Morocco.[33] The application of boring process in this complex operation involved a large special engineering machine for tunnel boring known as tunnel boring machine (TBM). In using TBM, it has been observed that several factors affect its operation. Robbins[34] stated that, it was always impossible to find a route that will avoid the problem of excavating in difficult geological zones with a sufficient degree of certainty. The extent and frequency of the difficulties encountered can be decisive in terms of economical viability or even in terms of the technical feasibility of a TBM drive. And in some cases, a very great potential damage, a single event can cast the entire project into doubt. The length and the number of critical stretches are very important in this respect. Short tunnel stretches with unfavorable but well-known geological conditions are not particularly risky for the economic success of a TBM drive provided that adequate countermeasures are planned in advance.[35]

TBM performance can be affected by geological conditions in a great variety of ways.[36] For instance, boreability problems in hard rock, steering difficulties or severe vibration of the cutter head due to mixed face or blocky rock conditions, major water inflows, cave-ins ahead of the tunnel face, or unstable excavation walls in highly fractured or weathered rock as well as crossing fault zones may represent difficult tunneling conditions. ITA[37] observed that squeezing ground conditions may also slow down or obstruct TBM operation and sometimes even call into question the feasibility of a TBM drive. Because of the nature of this complexity in mechanized tunneling, the need for well funded, thorough investigation of the risks, the technical feasibility, and the cost of TBM application cannot be overemphasized. Hence, it is not surprising that the question of TBM applicability in squeezing conditions has kept engineers busy for more than 30 years.[38–40] Due to the increased economic importance of mechanized tunneling associated with the demand for long-deep tunnels, the application of boring operation is particularly relevant today.

Ramoni and Anagnostou[41] carried out a comprehensive literature search on case histories involving TBMs under squeezing conditions in order to identify the specific problems associated with the use of TBMs. They observed that squeezing behavior may become problematic at different distances behind the tunnel face. Hence, the specific potential hazards concern both the machine area (sticking of the cutter head, jamming of the shield) and the back-up area (e.g., jamming of the back-up equipment, inadmissible convergences of the bored profile, damage to the tunnel support). In addition to the difficulties that are directly caused by squeezing behavior, adverse events such as clogging of the cutter head, insufficient bracing of the grippers, or instabilities of the face or the tunnel wall may also occur when boring through weak ground. It was equally difficult or even impossible to distinguish the different phenomena from each other. For example, when driving through poor-quality ground it may remain uncertain if the

Table 19   Surface roughness with passive damper (boring bar overhang length: 40 mm, depth of cut: 0.6 mm, and feed rate: 0.09 mm min^{-1})[28]

S/No	Speed (rpm)	Test No.	Vertical position			Test No.	Horizontal position		
			Response (surface finish R_a in μm)				Response (surface finish R_a in μm)		
			1	2	3		1	2	3
1	80	7	3.16	3.30	3.28	14	3.29	3.46	3.31
2	160	4	2.70	2.61	2.65	15	2.96	2.78	2.94
3	240	6	2.37	2.39	2.51	23	2.76	2.79	2.73

Table 20   Surface roughness with passive damper (boring bar overhang length: 80 mm, depth of cut: 0.6 mm, and feed rate: 0.09 mm min^{-1})[28]

S/No	Speed (rpm)	Test No.	Vertical position			Test No.	Horizontal position		
			Response (surface finish Ra in μm)				Response (surface finish Ra in μm)		
			1	2	3		1	2	3
1	80	1	2.61	2.40	2.50	16	3.14	3.27	3.35
2	160	8	2.56	2.37	2.31	21	2.38	2.47	2.71
3	240	9	2.61	2.40	2.50	22	1.26	1.38	1.56

Table 21   Surface roughness with passive damper (boring bar overhang length: 120 mm, depth of cut: 0.6 mm, and feed rate: 0.09 mm min^{-1})[28]
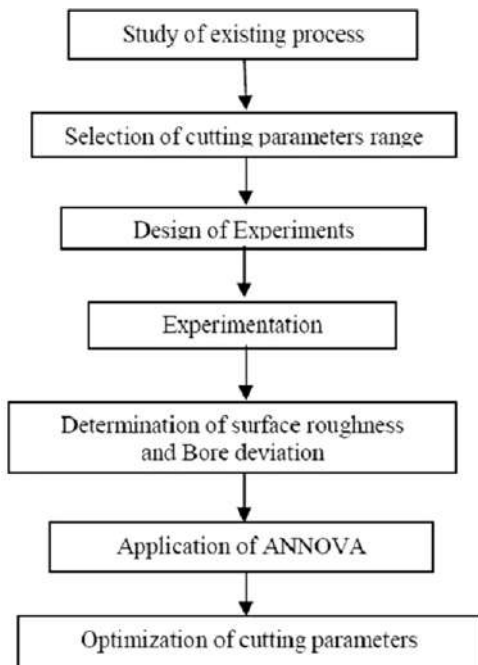
S/No	Speed (rpm)	Test No.	Vertical position			Test No.	Horizontal position		
			Response (surface finish Ra in μm)				Response (surface finish Ra in μm)		
			1	2	3		1	2	3
1	80	13	3.23	3.29	3.11	19	3.30	3.13	3.20
2	160	11	2.41	2.51	2.30	24	2.80	2.61	3.07
3	240	10	3.23	3.29	3.11	25	2.99	3.35	3.09

Figure 12   Flow Chart of Experimental Method.[29]

Table 22   Design of Experimental set up[29]

Run	Factor 1 (A)	Factor 2 (B)	Factor 3 (C)	Response
	Cutting allowance (mm)	Cutting speed (m min^{-1})	Feed rate (mm rev^{-1})	Bore deviation (μ)
1	0.3	120	0.1	0.017
2	0.5	120	0.1	0.022
3	0.3	140	0.1	0.02
4	0.5	140	0.1	0.019
5	0.3	160	0.1	0.018
6	0.5	160	0.1	0.02
7	0.3	120	0.2	0.021
8	0.5	120	0.2	0.021
9	0.3	140	0.2	0.02
10	0.5	140	0.2	0.021
11	0.3	160	0.2	0.016
12	0.5	160	0.2	0.019
13	0.3	120	0.3	0.023
14	0.5	120	0.3	0.022
15	0.3	140	0.3	0.021
16	0.5	140	0.3	0.021
17	0.3	160	0.3	0.014
18	0.5	160	0.3	0.015

Table 23   ANOVA for bore deviation[29]

Sources	Sum of square	df	Mean square	F-value	Desirability
Means vs. Total	6.806E-003	1	6.806E-003		
Linear vs. means	5.356E-005	3	1.785E-005	4.55	
2FI vs. Linear	3.146E-005	3	1.049E-005	4.92	Suggested
Quadratic vs. 2FI	7.556E-006	2	3.778E-006	2.14	Aliased
Residual	1.587E-005	9	1.764E-006		
Total	6.914E-005	18	17.59		

ground pressure acting upon the TBM is due to squeezing or raveling behavior.[35]

A marked difference exists between conventional and mechanized tunneling as a result of the magnitude of the potentially problematic deformations. Due to the geometrical constraints imposed by the equipment, even convergences as small as one or two decimeters may lead to difficulties in the machine or in the back-up area of a TBM drive Kovári.[42] Again, experience in some stretches of the Gotthard Base Tunnel has shown that hard but highly fractured rocks may also exhibit relevant deformations and challenge TBM tunneling, particularly if encountered at great depths. Tunneling experience shows that the ground deformations may develop very rapidly and very close to the working face. In such a situation, the achieved gross advance rate would play a secondary role (the TBM would become jammed even if operated at the highest feasible speed). Furthermore, standstills of TBM operation cannot be completely avoided.[39,43] Besides adverse ground conditions, unpredictable stops due to technical problems (e.g., electric power stoppages, mechanical breakdowns of the TBM, problems in the back-up system) have to be considered. For example, during the excavation of the Evinos–Mornos Tunnel (Greece) the cutter head of one of the gripper TBMs ($D=4.20$ m) became jammed during an excavation standstill which was caused by an interruption of the electric power supply.

When tunneling by a single shielded TBM (or a double shielded TBM in the so-called (auxiliary mode), the tunnel support (lining by precast segments) forms part of the thrusting system. There have been negative experiences in cases where a proper backfilling of the segmental lining was not achieved. For example, the double shielded TBM ($D=2.91$ m) that excavated a part of the Stillwater Tunnel (USA) probably became trapped in squeezing ground because of the impossibility of fully utilizing its installed thrust force. Firstly, it was not possible to drive the double shielded TBM in the 'gripper mode' and secondly, the improperly backfilled segmental lining was not able to withstand the combined loading of ground pressure and thrust force generated in the 'auxiliary mode.' In this case there was a further difficulty in relation to the telescopic part of the shield, which had a smaller diameter than the front and the rear shield, favoring the accumulation of loose material in this area, and thus leading to an increase in the friction that had to be overcome when moving the double shield. Similar problems also arose with gripper bracing, the backfilling of the segmental lining, and the telescopic part of the shield during the excavation of the Los Rosales tunnel (Colombia, double shielded TBM, $D=3.54$ m). Possible problems in the back-up area include inadmissible convergences of the bored profile or damage to the tunnel support. Such problems are basically the same as in conventional tunneling, the main differences being that in conventional tunneling (1) there is the option of excavating a considerably larger profile in the critical stretches (in order to accommodate the deformations) and (2) there is also more flexibility concerning the location of support installation (stabilization measures can be taken practically wherever and whenever required).

In TBM tunneling, the space available for ground deformations and tunnel support is largely predetermined by the fixed geometry of the excavated cross section. The possibility of enlarging the boring diameter locally is very limited (up to 30 cm, if at all possible). Besides the typical problems mentioned above, jamming of the back-up equipment is an additional hazard scenario to be considered, particularly for gripper TBMs. This has been experienced, for example, during the excavation of the Strada Section of the Tavanasa–Ilanz Tunnel (Switzerland, gripper TBM, $D=5.20$ m), in the Northern Section of the Vereina Tunnel (Switzerland, gripper-TBM, $D=7.64$ m), and, recently, in the Faido Section of the Gotthard Base Tunnel (Switzerland, gripper-TBM, $D=9.43$ m).

In furtherance of their research, Ramoni and Anagnostou[44] extensively studied the TBMs under squeezing conditions under the following subheadings:

1.2.3.1   Ground–Equipment–Support Interactions

They identified the relevant interfaces between the main system components and understanding their interactions was very important to an assessment of the critical situations. This might affect the performance, or even the feasibility of a TBM drive taking into consideration the peculiarities of existing TBM types with respect to thrusting systems, tunnel support, the presence or absence of a shield, and the achievable gross advance rate. They observed that the large number of interfaces between ground, tunneling equipment, and support in combination with the possibility of conflicting requirements and feedback effects introduces a high level of complexity, which necessitates an efficient mapping of the system and of its interfaces in order to identify and analyze the relevant interactions.

1.2.3.2   Boring and Thrusting

They have observed that the jamming of the TBM represents a major hazard as it may lead to serious damage, necessitating lengthy standstills for freeing or repairing the machine. Besides being important from a practical point of view, this potential problem is also theoretically very interesting and has attracted several research efforts over recent years. The researchers that have work in this area includes Graziani et al.,[45] Ramoni and Anagnostou,[46,47] and Sterpi and Gioda.[48] Ramoni and Anagnostou[44] further investigated the following conditions as it affects boring and thrusting.

1.2.3.2.1   Restart after standstill

If the ground behavior is time dependent, which is very common for squeezing conditions, a radial ground pressure may develop upon the machine during a standstill. In order to resume TBM operation, i.e., to move the TBM forwards and to rotate the cutter head, the thrusting system must be able to cope with the frictional forces acting upon the cutter head and the shield (**Figure 13**). In order to move the TBM forwards, both the installed thrust force and the bearing capacity of the thrusting system must be higher than the frictional resistance (static friction).

The frictional resistance was observed to increase with the radial pressure acting upon the machine (which may be high in the case of squeezing ground) and with the size of the loaded area (i.e., with the diameter and length of the cutter head and of the shield). However, it depends on the type of the ground and on the surface roughness of the cutter head and of the shield as they are relevant with respect to the skin friction coefficient.

1.2.3.2.2   Immobilization during ongoing excavation

TBM immobilization during the boring process can be seen as equivalent to the borderline case of a zero net advance rate. In the case of intensively squeezing ground, however, one should bear in mind that before the machine moves forwards the extrusion of the core has first to be compensated. Under normal conditions (characterized by the usual values for penetration and rotational speed), the effect of the core extrusion is small, but it may become relevant in the case of a low-penetration rate or a low-rotational speed. In extreme cases, the cutter head penetrates and rotates without moving forward (the penetration is used-up just for removing the axially deforming ground at the working face).

1.2.3.2.3   Tunnel support

Maidl *et al.*[49] stated that the application of tunnel support usually took place at two locations: in the machine area and later in the back-up area at a distance of 30–60 m behind the tunnel face. The locations of the support installation are determined by the design of the tunneling equipment. In the back-up area it is generally possible to install the tunnel support without slowing down the rate of TBM progress. Support application in the machine area, however, interferes considerably with TBM operation because, as a rule, it necessitates a halt of the machine. Furthermore, the support in the machine area may influence the ground pressure acting upon the shield. According to Schneider *et al.*,[50] particularly critical in this respect is the zone between the first and the second tunnel support installation points. In order to reduce the risk of problems in this area (e.g., jamming of the back-up equipment, inadmissible convergences of the bored profile, damage to the tunnel support) the installation of a higher quantity of tunnel support may be needed in the machine area, and this, as said before, will affect general TBM performance.

1.2.3.2.4   Single and double shielded TBMs

The differences between single and double shielded TBMs include the TBM length, the thrusting system, the tunnel support, and the advance rate. Single shielded TBMs are longer than gripper machines. As the area exposed to the squeezing pressure is larger, a higher frictional resistance has to be overcome and, consequently, all other parameters being equal, the risk of shield jamming is higher. The disadvantage of a longer shield is, nevertheless, not of absolute significance because single shielded TBMs usually have a higher installed thrust force than gripper TBMs.

1.2.3.3   Counter Measures

In order to influence system behavior, counter measures are as follows (1) cutter head, (2) geometry, (3) overboring, (4) shield, (5) thrust force and torque, (6) back-up equipment, and (7) tunnel support. While the tunnel support was studied under (1) practically rigid supports, (2) yielding supports, (3) deformable longitudinal joint elements, and (4) on the appropriate support concept.

In conclusion, the authors observed that, the result of a complex interaction between the ground, the tunneling equipment (TBM and back-up) and the support affect the TBM performance. Hence, the factors resulting from the three main
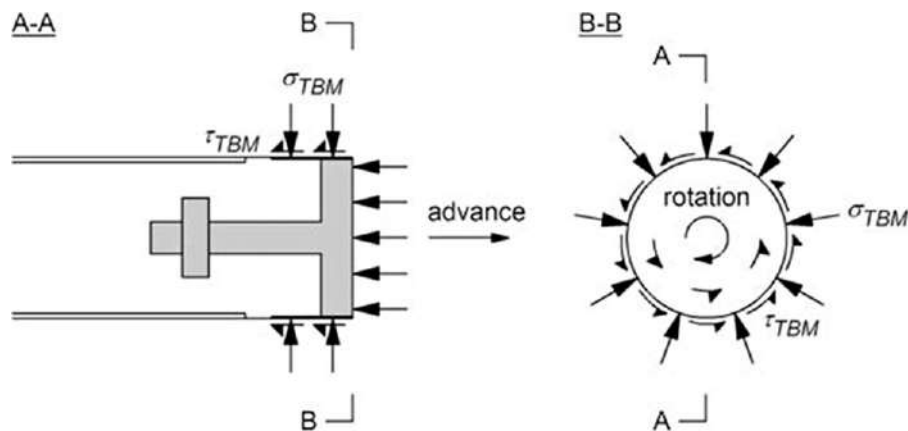
Figure 13   Loads acting on the TBM at restart (the shear and normal stresses at the face apply only in the case of a significant core extrusion). Ramoni, M.; Anagnostou, G. Tunnel Boring Machines under Squeezing Conditions. *Tunn. Undergr. SP. Technol.* **2010**, *25*, 139–157.

components of the system affect the TBM drive simultaneously and are usually coupled with each other.

Huo *et al.*[51] investigated the effect of disk cutters plane layout design of the full-face rock TBM based on different layout patterns. The study involved formulation of a nonlinear multi-objective mathematical model with multiple constraints for the disk cutters plane layout design, and analyses the characteristics of a multi-spiral layout pattern, a dynamic star layout pattern, and a stochastic layout pattern. The emphasis was put on the study of superiority of three different layout patterns as shown in **Figure 14**.

Different layout patterns were adopted in practice during the layout design of the disk cutters, while taken into consideration the engineering technical requirements and the corresponding structure design requirements of the cutter head. Genetic algorithm was employed to solve a disk cutter's multi-spiral layout problem and a cooperative coevolutionary genetic algorithm (CCGA) utilized to solve a disk cutter's star or stochastic layout problems. An instance of the disk cutter's plane layout design was solved by the proposed methods using three different kinds of layout patterns. Experimental results showed the effectiveness of the method of combining the mathematical model with the algorithms, and the pros and cons of the three layout patterns. Some of the observations made were as follows (1) the quality of plane layout design of the disk cutters for the full-face rock TBM directly affects the balance of force distribution on the cutter head during excavation, (2) the layout design of the disk cutters belongs to a complex optimization problem, so there was a need to make use of the advanced optimization methods to solve the problem, (3) the multi-spiral layout pattern can make the disk cutters distribute more evenly on the cutter head and can improve the stress distribution of the cutter head, and (4) the stochastic layout pattern can provide infinite possible solution space for the layout of the disk cutters and can produce the best solutions with the best performance indices.

1.2.4 Future Research Direction in Boring Operation

Available literatures in boring operation have shown a gap that needs to be investigated in order to fully appreciate how the various input factors affect the output factors or variables.

Studies have shown that cutting fluid types and method of its application could affect the outcome of an investigation during machining processes.[52,53] Efforts have been concentrated on how vibrations, ratio of length to diameter affects the results of boring operation and not much have been reported on how cutting fluids type or it methods of applications affect boring operation. Even when cutting fluids are used, it is never discussed as a factor that could affect the outcome of the result. For instance, Chang[54] used two nose radii in his work to evaluate the effect of vibrations on tool life and surface roughness. He found that surface roughness and tool wear were strongly affected by the vibration amplitude and frequency and that improper tool geometry and nose radius will produce more vibrations than the DOC. Huang and Chen[55] discovered that two types of vibrations may occur in machining, such as forced vibration and self excited vibration. Forced vibration was noted to be associated with bad gear drives, unbalanced machine-tool components, misalignment, or motors and pumps, etc., while self-excited vibration occurred due to chatter which was caused by the interaction of the chip removal process and the structure of the machine tool and resulted in disturbances in the cutting zone.

Similarly, Lin and Chang[56] studies show that vibrations have strong correlation with surface roughness, when effects of vibration signals on tool wear, surface quality, and machining time were studied. Bernardos and Vosniakos[57] investigated the relative motion between cutting tool and workpiece on the surface finish profile, using the ratio between vibration frequency and spindle rotational speed. While, Salgado *et al.*[58] studied the cutting parameters such as feed rate, spindle speed, DOC, tool nose radius, nose angle, and vibration data which are the input information for evaluation of tool life by adopting two levels of spindle speed, feed rate, and nose radius. Korkut and Kucuk[59] had proved that the best length to diameter ratio that results in less vibration in boring process is three. They obtained minimum vibration of tool and workpiece when the value of L/D ratio was taken as three. Tool failure in boring was identified by observing higher power consumption, poor surface finish, dimensional inaccuracy, appearance of a burnishing band on machined surface, tool vibrations, workpiece vibration, etc.

A lot of experimental and analytical studies have been employed to study boring bar dynamics and most researches

(a) Multi-spiral layout pattern   (b) Star layout pattern   (c) Stochastic layout pattern
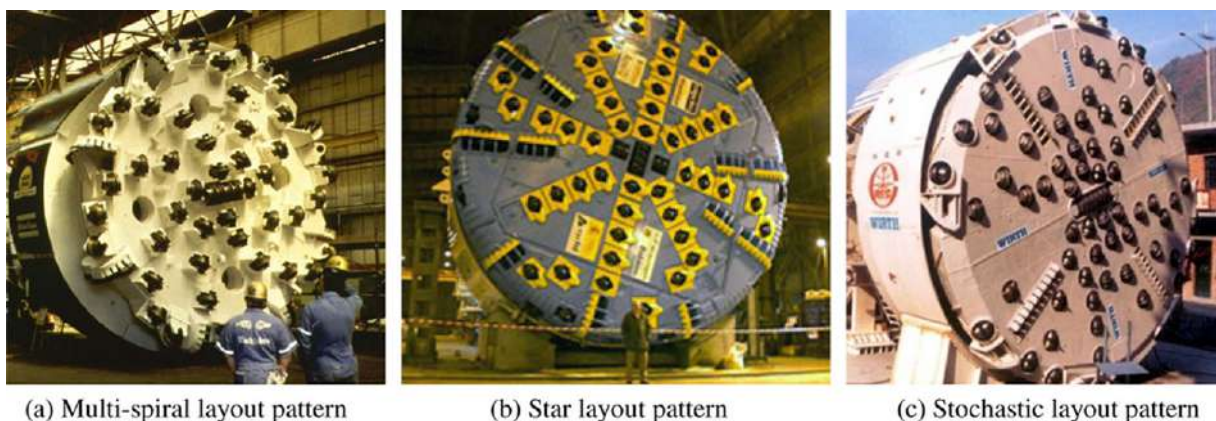
Figure 14 Different layout patterns of the disk cutters.[51]

were usually carried out on dynamic modeling of cutting dynamics and concentrated on the prediction of stability limits. Parker[60] investigated the stability limit of a slender boring bar in external longitudinal turning, experimenting with alternative regenerative cutting conditions at different cutting speeds and inclination angles. The vibration was measured in the cutting-speed and cutting-depth direction. He developed a two-degrees-of freedom analytical model of the boring bar with two input forces, one proportional to the variation of chip thickness and the other proportional to the penetration velocity. Based on boring bar point receptance estimates, the modal constants of the model were determined. Stability limits were predicted with the aid of the model; these were then compared with the experimental results. However, there was a wide range of cutting speeds resulting in extensive vibration in the cutting-speed direction, which was not predicted by the model. The experimental results indicated that the direction of vibration was either in the cutting-speed direction or in between the cutting speed and cutting depth direction.

Rao et al.[61] introduced an analytical dynamic boring force model which included the instantaneous variation of chip cross-sectional area under dynamic conditions. They produced a continuous system model of boring dynamics based on their dynamic boring force model and an uniform Euler–Bernoulli cantilever beam with a circular cross section. They studied boring with a zero side cutting edge angle and calculated chatter frequencies (fundamental eigen frequency of the boring bar) and amplitudes; these were then compared with the experimental results. They claim that their model correlates well with the experimental results.

Jayaram et al.[62] attempted to model the chatter stability limit in boring using a simplified analytical model of boring bar dynamics based on the direct point receptance functions and a linear regenerative cutting force model for three orthogonal directions. Jayaram et al.[40] claimed that estimates of the direct point receptances were produced based on hammer-excitation. Moreover, they experimentally determined stability limits for turning to validate their model. Kuster et al.[63] developed a computer simulation model of boring bar dynamics based on a three-dimensional model of regenerative cutting. Using the knowledge of the radius of curvature of the cutting tool tip as a base, their model differentiates between roughing and finishing in boring.

Marui et al.[64] investigated primary chatter of boring bars (with a rectangular cross section) and a tool holder shank using experiments in which they cut the top of a square thread in external longitudinal turning operations. The displacement of the boring bars was measured in both the cutting-speed and cutting-depth direction. With respect to the tool holder shank, both the cutting force and the displacement were measured in the cutting-speed direction. They used displacement and force as a function of time and chatter mark on the workpiece as well as displacement versus displacement to study primary chatter. They found that the vibration of the tool was dominating in the cutting-speed direction. The frequency of this self-excited vibration was slightly lower than the first natural frequency in the cutting-speed direction of both the boring bars and the tool holder shank. While, Taskesen[65] used a closed-loop feedback circuit in on-line vibration control

system to measure the relative vibration between workpiece and cutting tool. He used root mean square of workpiece vibration velocity to evaluate the tool life.

1.2.5   Conclusions

It has been established that one of the important factors that affect manufacturing cost is the cost of tooling; therefore any reduction in tooling cost will result in the reduction of manufacturing cost. This reduction in tooling cost can be achieved through proper selection of tool material, tool geometry, cutting speed, feed rate, DOC, and cutting fluids. Following the literature review on effect of cutting parameters during boring operation, it is observed that experimental investigation of the effect of cutting fluid types and its method of application in boring operation still remain an area of research that has not been studied.

Thus, it is of importance to investigate the effect of cutting fluids on the dynamic properties of the clamped boring bar, surface roughness, and tool wear during boring operation in order to gain further understanding of the dynamic behavior of clamped boring bars in the boring process. It is equally observed from literature that the TBM performance depends on a very complex interaction between the ground, the tunneling equipment (TBM and back-up), and the support. Hence, these factors resulting from the three main components of the system affect the TBM drive simultaneously and are usually coupled with each other.

References

1. Rao, K. V.; Murthy, B. S. N.; Rao, N. M. Cutting Tool Condition Monitoring By Analyzing Surface Roughness, Workpiece Vibration and Volume of Metal Removed for Aisi 1040 Steel in Boring. *Measurement* **2013**, *46*, 4075–4084.
2. Andren, L.; Håkansson, L.; Brandt, A.; Claesson, I. Identification of Dynamic Properties of Boring Bar Vibrations in a Continuous Boring Operation. *Mech. Syst. Signal Process.* **2004**, *18* (4), 869–901.
3. Andren, L.; Håkansson, L.; Brandt, A.; Claesson, I. Identification of Motion of Cutting Tool Vibration in a Continuous Boring Operation – Correlation to Structural Properties. *Mech. Syst. Signal Process.* **2004**, *18* (4), 903–927.
4. Tobias, S. A. *Machine Tool Vibration*; Blackie: London, 1965.
5. Kato, S.; Marui, E. On the Cause of Regenerative Chatter Due to Workpiece Deflection. *J. Eng. Ind.* **1974**, *96* (1), 179–186.
6. Khraisheh, M. K.; Pezeshki, C.; Bayoumi, A. E. Time Series Based Analysis for Primary Chatter in Metal Cutting. *J. Sound. Vib.* **1995**, *180* (1), 67–87.
7. Hamdan, M. N.; Bayoumi, A. E. An Approach to Study the Effects of Tool Geometry on the Primary Chatter Vibration in Orthogonal Cutting. *J. Sound. Vib.* **1989**, *128* (3), 451–469.
8. Sturesson, P.-O. H.; Hakansson, L.; Claesson, I. Identification of the Statistical Properties of the Cutting Tool Vibration in a Continuous Turning Operation–Correlation to Structural Properties. *J. Mech. Syst. Signal. Process.* **1997**, *11* (3), 459–489.
9. Tlusty, J. Analysis of the State of Research in Cutting Dynamics. *Ann. CIRP* **1978**, *27*, 583–589.
10. Scheuer, J.; Kansson, L.H.; Claesson, I. Modal Analysis of a Boring Bar using Different Clamping Conditions. In *Proceedings of the Eleventh International Congress on Sound and Vibration*; ICSV11: St. Petersburg, Russia, 2004.

11. Arnold, R. N. Mechanism of Tool Vibration in Cutting of Steel. *Proc. Inst. Mech. Eng.* **1946**, *154* (1), 261–284.

12. Merritt, H. E. Theory of Self-Excited Machine-Tool Chatter, Contribution to Machine-Tool Chatter, Research–1. *J. Eng. Ind., Trans. ASME* **1965**, *87* (4), 447–454.

13. Thompson, R. A. The Modulation of Chatter Vibrations. *J. Eng. Ind.* **1969**, *91* (3), 673–677.

14. Akesson, H.; Smirnova, T.; Hakansson, L. Analysis of Dynamic Properties of Boring Bars Concerning Different Clamping Conditions. *Mech. Syst. Signal. Pr.* **2009**, *23*, 2629–2647.

15. Saindane, G.; Jakikore, A.; Umbarkar, A. Experimental Investigation of Vibration Damping in Boring Operation Using Passive Damper. *Int. J. Res Eng. Adv. Technol.* **2014**, *2* (3), 1–3.

16. Khatake, P.; Nitnaware, P. T. Vibration Mitigation Using Passive Damper in Machining. *Int. J. Mod. Eng. Res. Technol.* **2013**, *3* (6), 3649–3652.

17. Kadu, R. S.; Awari, G. K.; Sakhale, C. N.; Modak, J. P. Formulation of Mathematical Model for the Investigation of Tool Wears in Boring Machining Operation on Cast Iron Using Carbide and CBN Tools, 3rd International Conference on Materials Processing and Characterisation (ICMPC 2014). *Procedia Mater. Sci.* **2014**, *6*, 1710–1724.

18. Schenck, H., Jr. *Theory of Engineering Experimentation*; Mc Graw Hill: New York, NY, 1961.

19. Modak, J. P.; Bapat, A. R. Formulation of Generalised Experimental Model for a Manually Driven Flywheel Motor and Its Optimization. *Appl. Ergon.* **1994**, *25* (2), 119–122.

20. Badadhe, A. M.; Bhave, S. Y.; Navale, L. G. Optimization of Cutting Parameters in Boring Operation. *IOSR J. Mech. Civ. Eng.* **2005**, *2320–334X*, 10–15.

21. Moetakef-Imani, B.; Yussefian, N. Z. Dynamic Simulation of Boring Process. *Int. J. Mach. Tool. Manu.* **2009**, *49*, 1096–1103.

22. Yussefian, N. Z.; Moetakef-Imani, B.; El-Mounayri, H. The Prediction of Cutting Force for Boring Process. *Int. J. Mach. Tool. Manu.* **2008**, *48*, 1387–1394.

23. Lazoglu, I.; Atabey, F.; Altintas, Y. Dynamics of Boring Processes: Part III – Time Domain Modeling. *Int. J. Mach. Tool. Manu. 42* **2002**, *42*, 1567–1576.

24. Komanduri, R.; Lee, M.; Raff, L. M. The Significance of Normal Rake in Oblique Machining. *Int. J. Mach. Tool. Manu.* **2004**, *44*, 1115–1124.

25. Min, B. K.; O'Neal, G.; Koren, Y.; Pasek, Z. A Smart Boring Tool for Process Control. *Mechatronics* **2002**, *12*, 1097–1114.

26. Koren, Y.; Ko, T. R.; Ulsoy, A. G. Tool Wear Estimation Under Varying Cutting Conditions. *Trans ASME, J. Dyn. Syst. Control* **1991**, *113* (2), 300–307.

27. Shiraishi, M. Scope of In-Process Measurement, Monitoring and Control Techniques in Machining Processes – Part 1: In-Process Techniques for Tools. *Precis. Eng.* **1988**, *10* (4), 179–189.

28. Kanase Sandip, S.; Patil Jaydeep, S.; Jadhav Sainand, M. Improvement of Ra Value of Boring Operation Using Passive Damper. *Int. J. Eng. Sci.* **2013**, *2* (7), 103–108.

29. Kumar, P.; Oberoi, J. S.; Singh, C.; Dhiman, H. Analysis and Optimization of Parameters Affecting Bore Deviation in Boring Process. *Int. J. Innov. Tech. Res.* **2014**, *2* (3), 967–972.

30. Kovári, K. The Two Base Tunnels of the Alptransit Project: Lötschberg and Gotthard. In *Worldwide Innovations in Tunnelling, STUVA-Tagung '95, Stuttgart, Forschung + Praxis 36*. Alba Fachverlag GmbH + Co.KG: Düsseldorf, 1995; pp. 23–29.

31. Bergmeister, K. Brenner Base Tunnel: Link Between Munich and Verona. *Tunnel* **2007**, *1/2007*, 9–20.

32. Nasri, V.; Fauvel, P. Lyon-Turin Long and Deep Railway Tunnel Project. In *Rapid Excavation and Tunnelling Conference*, SME IncSeattle: Littleton, CO, 2005; pp. 531–543.

33. Pliego, J. M. Open Session – The Gibraltar Strait Tunnel. An Overview of the Study Process. *Tunn. Undergr. SP. Technol.* **2005**, *20* (6), 558–569.

34. Robbins, R. J. Large Diameter Hard Rock Boring Machines: State of the Art and Development in View of Alpine Base Tunnels. *Felsbau* **1992**, *10* (2), 56–62.

35. Kovári, K. Rock Deformation Problems When using Full-Facing Cutting Equipment in Rock, Part 1. *Tunnel* **1986**, *3/86*, 236–244.

36. Barla, G.; Pelizza, S. TBM Tunnelling in Difficult Ground Conditions. In *GeoEng2000 – International Conference on Geotechnical & Geological Engineering, Melbourne*; Vol. 1; Technomic Publishing Company Inc.: Lancaster, 2000; 1471–1489.

37. ITA. Long Traffic Tunnels at Great Depth. In *ITA Working Group N-17 – Long Tunnels at Great Depth*; ITA: Lausanne, 2003.

38. Prader, D. Beispiele von Druckerscheinungen im Tunnelbau. In *Internationales Symposium für Untertagbau, Luzern, Schweizerische Gesellschaft für Boden– und Felsmechanik Zürich*; 1972; pp. 82–98.

39. Lombardi, G. Bau von Tunneln bei grossen Verformungen des Gebirges. In *Tunnel 81, Internationaler Kongress, Düsseldorf, Band 2, Messegesellschaft mbH NOEWA Düsseldorf und Deutsche Gesellschaft für Erd – und Grundbau e.V. Essen*, 1981; pp. 351–384.

40. Robbins, R.J. The Application of Tunnel Boring Machines to Bad Rock Conditions. In *Rock Mechanics: Caverns and Pressure Shafts, ISRM Symposium, Aachen*, Vol. 2; A.A. Balkema: Rotterdam, 1982; pp. 827–836.

41. Ramoni, M.; Anagnostou, G. Experiences and Basic Considerations on TBM Tunnelling in Squeezing Ground. In *Research Project FGU 2007/005, Report 090201 (Revision B) of the Institute of Geotechnical Engineering (IGT) of the ETH Zurich to the Swiss Federal Roads Office (FEDRO)*, 2009.

42. Kovári, K. Rock Deformation Problems When using Full-Facing Cutting Equipment in Rock, Part 2. *Tunnel* **1986**, *4/86*, 289–298.

43. Gehring, K. H. Design Criteria for TBM's with Respect to Real Rock Pressure. In *Tunnel Boring Machines – Trends in Design & Construction of Mechanized Tunnelling, International Lecture Series TBM Tunnelling Trends*, Hagenberg, A.A. Balkema, Rotterdam, Brookfield, 1996; pp. 43–53.

44. Ramoni, M.; Anagnostou, G. Tunnel Boring Machines under Squeezing Conditions. *Tunn. Undergr. SP. Technol.* **2010**, *25*, 139–157.

45. Graziani, A.; Capata, A.; Romualdi, P. Analysis of Rock-TBM-Lining Interaction in Squeezing Rock. *Felsbau Magazin* **2007**, *25* (6), 23–31.

46. Ramoni, M.; Anagnostou, G. The Effect of Advance Rate on Shield Loading in Squeezing Ground. In *Underground Space – The 4th Dimension of Metropolises, ITA World Tunnel Congress 2007, Prague*, Vol. 1, 2007a; Taylor & Francis Group: London; pp. 673–677.

47. Ramoni, M.; Anagnostou, G. Numerical Analysis of the Development of Squeezing Pressure During TBM Standstills. In *The Second Half Century of Rock Mechanics, 11th Congress of the International Society for Rock Mechanics (ISRM), Lisbon*, Vol. 2, 2007b; Taylor & Francis Group: London; pp. 963–966.

48. Sterpi, D.; Gioda, G. Ground Pressure and Convergence for TBM Driven Tunnels in Visco-Plastic Rocks. In *ECCOMAS Thematic Conference on Computational Methods in Tunnelling, EURO:TUN 2007*; Vienna University of Technology, 2007; p. 89.

49. Maidl, B.; Schmid, L. R.; Ritz, W.; Herrenknecht, M. *Tunnelbohrmaschinen im Hartgestein*; Ernst & Sohn Verlag für Architektur und technische Wissenschaften GmbH: Berlin, 2001.

50. Schneider, E.; Home, L.; Sänger, B.; Kolb, S. Innovative Concept for Constructing the Brenner Base Tunnel with Previously Produced Exploratory Tunnel. *Tunnel* **2007**, *1/2007*, 21–33.

51. Junzhou Huo; Wei Sun; Jing Chen; Xu Zhang. Disc Cutters Plane Layout Design of the Full-Face Rock Tunnel Boring Machine (TBM) Based on Different Layout Patterns. *Comput Ind Eng* **2011**, *61*, 1209–1225.

52. Lawal, S. A.; Choudhury, I. A.; Nukman, Y. Application of Vegetable Oil-Based Metalworking Fluids in Machining Ferrous Metals – A Review. *Int. J. Mach. Tool. Manu.* **2012**, *52*, 1–12.

53. Lawal, S. A.; Choudhury, I. A.; Nukman, Y. A Critical Assessment of Lubrication Techniques in Machining Processes: A Case for Minimum Quantity Lubrication Using Vegetable Oil-Based Lubricant. *J. Clean. Prod.* **2013**, *41*, 210–221.

54. Chang, F. X. An Experimental Study of the Impact of Turning Parameters on Surface Roughness. In *Proceedings of the Industrial Engineering Research Conference, Paper No. 2036, GA*, 2001.

55. Huang, L. H.; Chen, J. C. A Multiple Regression Model to Predict In-Process Surface Roughness in Turning Operation via Accelerometer. *J. Ind. Technol.* **2001**, *17* (2), 2–7.

56. Lin, C. S.; Chang, F. M. A Study on the Effects of Vibrations on the Surface Finish using a Surface Topography Simulation Model for Turning. *Int. J. Mach. Tool. Manu.* **1998**, *38* (7), 763–778.

57. Bernardos, P. G.; Vosniakos, G. C. Predicting Surface Roughness in Machining: A Review. *Int. J. Mach. Tool. Manu.* **2003**, *43*, 833–844.

58. Salgado, D. R.; Alonso, F. J.; Cambero, I.; Marcelo, A. In-Process Surface Roughness Prediction System using Cutting Vibrations in Turning. *Int. J. Adv. Manuf. Tech.* **2009**, *43*, 40–51.

59. Ihsan Korkut; Yilmaz Kucuk. Experimental Analysis of the Deviation from Circularity of Bored Hole Based on the Taguchi Method. *J. Mech. Eng.* **2010**, *56* (5), 340–346.

60. Parker, E. W. Dynamic Stability of a Cantilever Boring Bar with Machined Flats Under Regenerative Cutting Conditions. *J. Mech. Eng. Sci.* **1970**, *12* (2), 104–115.

61. Rao, P. N.; Rao, U. R. K.; Rao, J. S. Towards Improved Design of Boring Bars Part 1: Dynamic Cutting Force Model with Continuous System Analysis for the Boring Bar. *Int. J. Mach. Tool. Manu.* **1988**, *28* (1), 33–44.

62. Jayaram, S.; Iyer, M. An Analytical Model for Prediction of Chatter Stability in Boring. *Trans. NAMRI/SME* **2000**, *28*, 203–208.

63. Kuster, F. Cutting Dynamics and Stability of Boring Bars. *Ann. CIRP* **1990**, *39* (1), 361–366.

64. Marui, E.; Ema, S.; Kato, S. Chatter Vibration of Lathe Tools. Part 1: General Characteristics of Chatter Vibration. *J. Eng. Ind., Trans. ASME* **1983**, *105*, 100–106.

65. Taskesen, A. Computer Aided Nonlinear Analysis of Machine Tool Vibrations and Developed Computer Software. *Math. Comput. Appl* **2005**, *3*, 377–385.